ELSEVIER

Journal of Nuclear Materials 241–243 (1997) 316–321

journal of nuclear materials

Impurity fueling to terminate Tokamak discharges

S. Putvinski [a,*], N. Fujisawa [a], D. Post [a], N. Putvinskaya [b], M.N. Rosenbluth [a], J. Wesley [a]

[a] *ITER Joint Central Team, 11025 N. Torrey Pines Rd., La Jolla, CA 92037, USA*
[b] *SAIC, 11025 N. Torrey Pines Rd., La Jolla, CA 92037,, USA*

Abstract

A model has been developed to investigate the requirements for terminating ITER discharges by introducing large quantities of either hydrogen or impurities to radiate the energy and quench the discharge before the discharge can undergo substantial motion and come into contact with the wall. The results of the model indicate that the injection of impurities will lead to runaway currents as large as 60% of the initial plasma current. Injection of hydrogen or low Z impurities is more hopeful, but even they can cause runaways. Radiation transport effects will likely be very important.

Keywords: ITER; Disruptions; 1D model; Impurity source; Radiation energy sink

1. Introduction

Development of fast plasma shutdown scenarios for ITER is an important aspect of ITER physics design and operation planning. The reasons why a fast shutdown capability is needed include (1) termination of uncontrolled fusion power increases (burn control failure), (2) limitation of the thermal consequences of PF control failures that result in plasma mispositioning relative to the first wall or divertor channel/targets, (3) mitigation of disruption erosion of the divertor target surfaces and (4) mitigation of the severity of the thermal and electromagnetic loading consequences of vertical displacement events (VDEs). To avoid damage of the respective plasma-facing-component surfaces, the fast shutdown system must be able terminate the fusion power and remove the plasma thermal energy faster than 3 s [1]. Minimum and maximum shutdown requirements for ITER are summarized in Table 1.

Injection of impurities was proposed as a candidate for the fast plasma shutdown in ITER [1,2]. Impurity radiation can provide the required termination time and distribute the plasma thermal and magnetic energy over the large first wall surface area. The impurity can be injected as solid pellets or a massive gas puff. Injection of compact toroids is also considered as a candidate for delivering impurities to the plasma center [4]. Impurity pellet injection has been tested in the present experiments and initial experimental results are encouraging.

The paper presents the results of 1D modeling of fast plasma termination by impurity injection carried out in order to study the phenomena accompanying discharge termination in ITER and develop specifications for the shut down system. An important part of the model is simulation of runaway electrons which impose a very strict limitation on the kind of impurity and the parameters of the pellets.

2. Model description

We used a simple plasma geometry, a straight, circular cylinder ($r < a$) surrounded by a thin conducting wall with a finite resistivity. The model includes a 1D equation for

* Corresponding author. Tel.: 1-619 622 5164; fax: 1-619 546 8602.

PII S0022-3115(96)00521-1

Table 1
Maximum and minimum thermal and current quench times

	Minimum	Maximum
Thermal quench time, t_{TH} (s)	0.01 (melting of the surface layer of the first wall)	3 (to avoid local melting of the plasma facing components)
Current quench time, t_C (s)	0.02 (large local mechanical loads on blanket modules)	3 (upper estimation for VDE time)

the plasma energy balance, Ohm's law and Maxwell equation for the evolution of the toroidal electric field.

$$\frac{\partial W}{\partial t} = \frac{1}{r}\frac{\partial}{\partial r}\kappa r\frac{\partial T}{\partial r} + P_{fus} + P_{OH} - P_{Rad} \quad (1)$$

$$j_\varphi = j_{RA} + \sigma E \quad (2)$$

$$\frac{\partial j_\varphi}{\partial t} = \frac{c^2}{4\pi}\frac{1}{r}\frac{\partial}{\partial r}r\frac{\partial E}{\partial r} \quad (3)$$

where $W = \frac{3}{2}(n_e + n_{DT} + n_Z)T$ is the total plasma energy, P_{fus} is the alpha-particle heating power, P_{OH} is the Ohmic heating power, P_{Rad} is the radiation loss, κ is the plasma thermal conductivity and σ is the neoclassical plasma conductivity [3], j_{RA} is the current density produced by runaway electrons. We assume equal temperatures for all plasma species in the power balance equation. The radiation loss consists of two terms: bremsstrahlung and impurity line radiation, $P_{Rad} = P_B + P_L$. For impurity line radiation we used coronal equilibrium values [5] after testing a time dependent model with individual charge states and determining that coronal equilibrium was adequate.

$$P_L = n_e n_Z L(T) \quad (4)$$

where $n_e = n_{DT} + \langle Z\rangle n_Z$, n_{DT} is the DT ion density and n_Z is the impurity ion density and $\langle Z\rangle$ is a function of the plasma temperature. A detailed collisional radiative model is used for hydrogen recombination and radiation [5]. The electric field at the plasma edge was derived from a circuit equation including eddy currents in the resistive wall, J_w:

$$\dot{J}_p + \dot{J}_w = -J_w/\tau_w \quad (5)$$

Here $\tau_w = L_w/R_w$ is the resistive decay time for currents in the wall.

The current produced by runaway electrons is described by a simple model derived from the Fokker–Plank equation for relativistic electrons:

$$\frac{\partial j_{RA}}{\partial t} = \frac{j_{RA}}{\tau_{RA}}\left(\frac{E}{E_c} - 1\right) + S \quad (6)$$

where

$$\frac{1}{\tau_{RA}} = \frac{4\pi e^4 n_T}{m^2 c^3}\sqrt{\frac{\pi}{3(Z_{eff}+5)}};$$

$$E_c = \frac{2\pi e^3(n_e + n_T)}{mc^2}\ln\lambda \quad (7)$$

n_T is the total electron density (free and bound), $n_T = n_{DT} + Zn_Z$. The first term in the right hand side describes the avalanche of runaway electrons due to large angle Coulomb collisions. The avalanche effect can exist when the electric field is larger than the critical field, E_c, defined by Eq. (7) and is equal to the minimum drag force acting on a runaway electron in the plasma which occurs at the electron energy $\sim mc^2$. The sum $n_e + n_T$ in Eq. (7) takes into account a factor of 2 difference in the Coulomb logarithm for free and bound electrons. For ITER conditions, the avalanche produces a very large amplification of the initial current $j \approx j(0)\exp(2.5I\ (\mathrm{MA}))$. It is therefore crucial to take into account all of the important sources of runaways. Different sources of runaway electrons (including Dreicer acceleration, high energy tails remaining from the early pre-cooled stages of the plasma, tritium beta decay and radiation from the activated first wall) have been analyzed. Among all these sources, we found that the most important for ITER conditions is MeV γ-ray emission from the activated ITER first wall. The large avalanche amplification factor defines the conditions necessary for the absence of runaways in ITER:

$$E\ (\mathrm{V/m}) < E_c \approx 0.05\frac{(n_e + n_T)}{10^{20}\ (\mathrm{m}^{-3})}.$$

We did not specify a means for delivery of impurities to the plasma core. Instead we prescribed an initial impurity profile together with the initial plasma profiles and followed the evolution of the plasma temperature and current profiles. We assumed that plasma ion and impurity density profiles do not change during the plasma shutdown. To avoid formation of very peaked current profiles during the plasma evolution and to simulate MHD activity in cases where q dropped below 1, we increased the thermal conductivity, κ, by a factor of 10^3 above the nominal value in the region where the safety factor, q, fell below 1.

We developed a one dimensional transport code to solve the above equations. The code was first validated using present experimental results.

3. Results of the modeling

We modeled the injection of deuterium and different impurities such as Xe, Ne, Be and He and varied the amount of injected material. All of the results presented below were obtained for the reference ITER parameters [1].

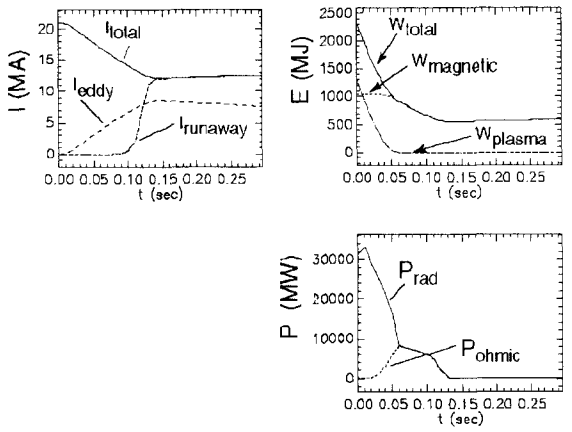

Fig. 1. Time traces of plasma global parameters after injection of 1% of Xe. W_{th} – thermal energy, W_m – magnetic energy, I_p – plasma current, I_{RA} – current of runaway electrons, P_{OH} – Ohmic heating power, P_{Rad} – plasma radiation power.

We found that the evolution of the plasma profiles after impurity injection occurs in two phases: a thermal energy collapse and a current quench. An example is shown in Figs. 1 and 2 where the time history of the plasma current and energy after the injection of 1% of Xe are shown. The thermal energy collapse starts from the plasma edge where the plasma temperature is low and the line radiation is strongest. In a few ms, a radiating shell is formed and starts moving from the edge to the plasma center leaving behind a cold plasma. If the impurity concentration is large enough, the cooling front moves rapidly and the current profile does not change much except for a thin skin current moving with the front. The results presented in Figs. 1 and 2 were obtained with a uniform Xe profile.

After 50 ms, the cooling front reaches the plasma center. The temperature of the post-thermal quench plasma is about 10 eV, the plasma has a high resisitivity and the loop voltage increases up to 500 V which is far greater than the critical field (Eq. (7)) for runaway formation. The second phase is characterized by the evolution of the plasma current for an almost constant plasma temperature of about 10 eV which is maintained by the energy balance between impurity radiation and Ohmic heating.

During the next 50 ms the plasma current continues to decay which causes eddy currents in the wall. At $t = t_{cur} \approx 110$ ms, the runaway current replaces the resistive current and the electric field reduces to the critical field of about 0.1 V/m. As a result, the Ohmic heating is reduced and the plasma temperature decreases to about 1 eV. Further evolution for the current and temperature is very slow and the runaway current is sustained in the plasma for a few tens of seconds. The runaway current slowly increases due to the decay of the eddy current in the wall. The runaway current has approximately the same current density at the plasma center as the initial current density but a more narrow radial profile.

Xe injection leads to the generation of a significant runaway current for practically any Xe density (Figs. 3 and 4). In the range of interest, $n_{Xe} = 10^{17}$–2×10^{18} m^{-3}, the runaway current will exist in the plasma for many tens of seconds and will interact with the first wall after the development of a VDE. Fig. 4 shows the magnitude of the runaway current at $t = t_{cur}$. After this point, a part of the eddy current will be also transformed to the runaway current and the maximum value of runaway current could be larger than shown in Fig. 4. However, the VDE which will likely follow the thermal quench will terminate this process before full decay of the eddy current.

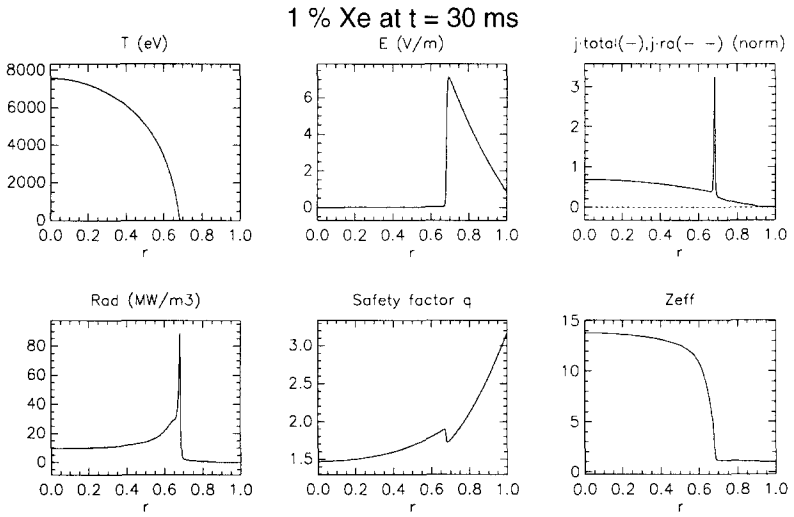

Fig. 2. Plasma profiles at $t = 30$ ms after injection of 1% Xe. Uniform distribution of Xe density. Initial plasma profiles and parameters correspond to the reference plasma scenario, $\langle n \rangle = 1.04 \times 10^{20}$ m^{-3}, $\langle T \rangle = 11$ keV, $I_p = 21$ MA.

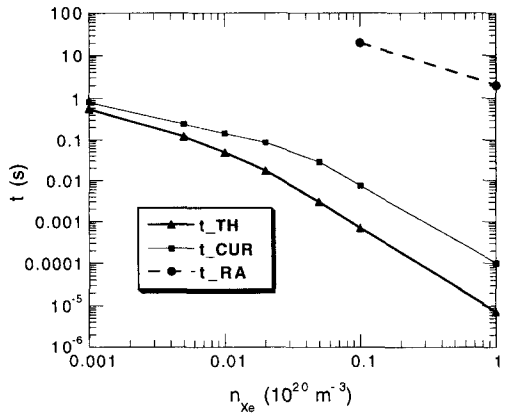

Fig. 3. Thermal quench time, resistive current quench time, runaway current decay time as function of the Xe density.

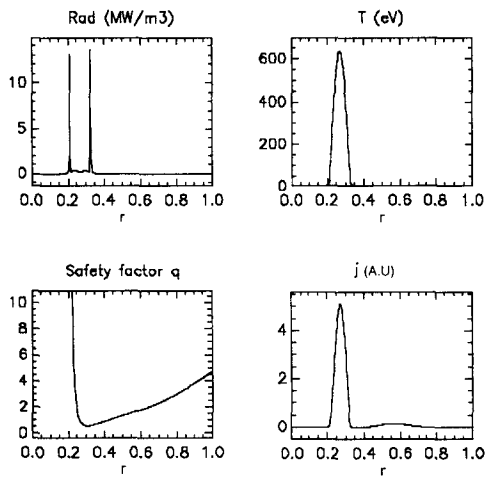

Fig. 5. Plasma profile formed at $t = 3.5$ s after injection of 1.5% of Ne in ITER plasma.

Sometimes instead of formation of runaway electrons, we observed another phenomena which extends the current quench and delays formation of runaway electrons. Due to a thermal instability, the plasma temperature and current profile break down into several narrow layers which are embedded in the cold and currentless plasma. The soliton type spikes have maximum temperature about a few hundred eV and low resistivity and persist for a long time disappearing one after another. An example is presented in Fig. 5. which shows the plasma profiles formed after injection of 1.5% of Ne in ITER plasma. The Ohmic heating power is transported by thermal conductivity to the low temperature region where it is radiated by Ne impurity.

Similar soliton type solutions can be observed even with only bremsstrahlung radiation and no line radiation in the hydrogen plasma. In this case we can give a simple analytical description for these type of the profiles. We assume that the temperature profile is narrow and neglect the variation of the electric field across the layer. Neglecting also the alpha-particle heating we can rewrite Eq. (1) as follows:

$$\chi n_e \frac{\partial^2 T}{\partial r^2} + C_{OH} E^2 T^{3/2} - C_B n_e^2 T^{1/2} = 0 \qquad (8)$$

where $C_{OH} = \sigma/T^{3/2} = \text{constant}$ and $C_B = 1.69 \times 10^{-32}$ (W m^3/eV$^{1/2}$). Eq. (8) can be integrated once which gives:

$$\tfrac{1}{2}\left(\frac{\partial T}{\partial r}\right)^2 + U(T) = E_0 \qquad (9)$$

The 'potential' $U(T) \propto T^{3/2}(T - T_m)$, where $T_m = 5C_B n_e^2/3C_{OH}E^2$ is shown in Fig. 6. Using a mechanical analogy of the motion in a potential well one can see that at $E_0 = 0$, Eq. (9) has a soliton type solution with $T \to 0$ at $r \to \pm\infty$. Bremsstrahlung was used here as an example.

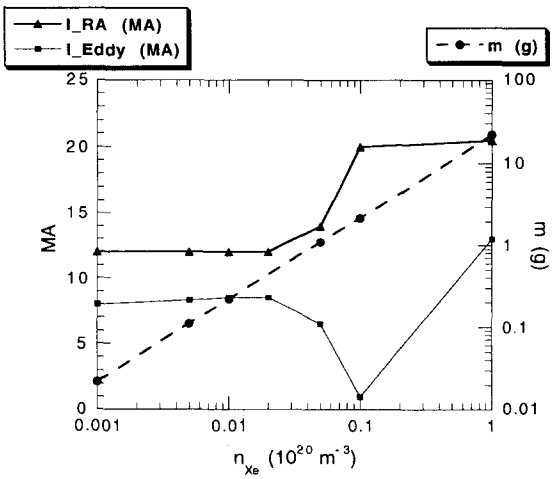

Fig. 4. Magnitude of the runaway and maximum eddy current as function of the Xe density. Total mass of Xe impurity is also shown.

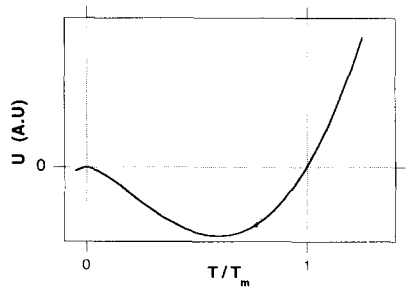

Fig. 6. U as function of T/T_m.

The same type of solutions exist in the case of impurity line radiation. Solitons are produced during radiative cooling within a given range of impurity density and are stable to 1D perturbations.

Filamentation of the current profile can only delay the formation of runaways in ITER conditions. Even in the case of the low impurity level shown in Fig. 5, the runaway current shows up as a broad peak at $r = 0.55$. Later, the soliton disappears and the runaway current will grow up to about 50% of the initial plasma current.

The simulations show that runaway electrons always form after injection of any high Z impurity such as Xe, Ar or Ne. We found that even Be injection produces runaway electrons in ITER. However, when the Z of the impurity is reduced, larger amounts of injected impurity are required and the electron density after injection is higher. As a result the critical electric field increases and the plasma becomes less susceptible to runaway formation. We therefore investigated deuterium as a candidate for plasma shutdown.

Fig. 7 shows the thermal and current quench time as function of the added deuterium density. It can be seen that the required range of quench times corresponds to a density range of $2\text{–}10 \times 10^{21}$ m^{-3}. Because of the high electron density, the decay time for the runaway current is less than a few seconds. The main channel of plasma energy loss at temperatures above 50 eV is bremsstrahlung radiation which at this high density provides very fast plasma cooling. There is some uncertainty as to the final plasma temperature. If we assume that the plasma is transparent to line radiation, then the final temperature will be very low and a large fraction of D ions will recombine. For a plasma density of $2\text{–}10 \times 10^{21}$ m^{-3} the equilibrium neutral density will be high enough to absorb fully the L_α and other hydrogen line radiation. For neutral densities of $\sim 10^{22}$ m^{-3}, the mean free path for L_α radiation is 2×10^{-5} m. We have not yet developed a radiation model adequate to investigate the consequences of radiation trapping so we calculated two limiting cases: one with line radiation and bremsstrahlung and one with only bremsstrahlung radiation. In the case with no line radiation, we did not observe runaway electrons for any deuterium density of interest. This is illustrated in Fig. 8 which shows the maximum eddy current and runaway current as a function of the deuterium density. The temperature after the thermal quench is large enough to keep the electric field below the critical field which is as high as 5–10 V/m for this density range.

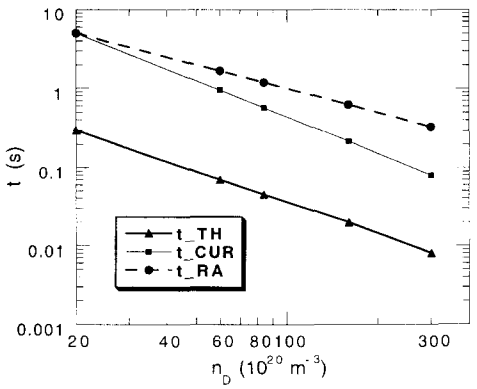

Fig. 7. Thermal quench time, resistive current quench time, runaway current decay time as function of D density.

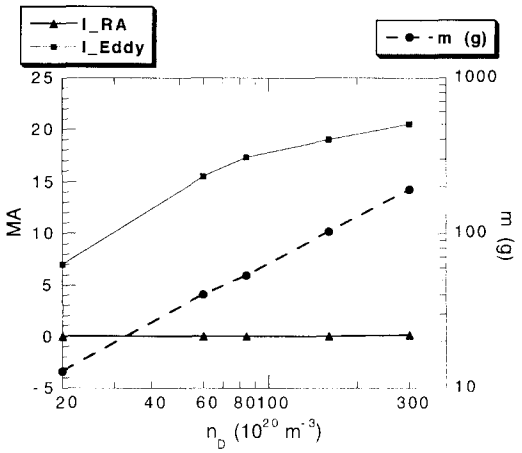

Fig. 8. Magnitude of the runaway and eddy current as function of D density. The total mass of injected D is also shown. No line radiation is included.

Addition of line radiation to our model reduces the post-thermal quench temperature to a few eV and as a result increases the electric field above the critical value. In this case, runaway electrons were absent only at low density. For deuterium densities above 2×10^{21} m^{-3}, we observed a few MA's of runaway current which died away after 1–2 s. However, the plasma at the edge fully recombines long before the runaway current is generated. This may lock the line radiation within the plasma and, as a result, increase the plasma temperature. It is thus likely that a more accurate radiation model will increase the density limit for runaway formation.

4. Conclusions

Modeling the fast termination of the ITER plasma shows that impurity pellet injection can remove the plasma thermal energy and reduce the plasma current sufficiently during the required time presented in the Table 1. However, our model indicates that the presence of high Z impurities in the plasma leads to the formation of large runaway currents (50–75% of initial current) which are potentially dangerous for the first wall.

A more attractive solution is the massive injection of a low Z material such as D or He which makes the plasma much less susceptible to runaway electron formation and at the same time can provide the required termination times. The required amount of deuterium is 20–100 g. Estimates indicate that it may be feasible to deliver 50 g of solid D to the center of ITER plasmas with a train of 50 of 1 g pellets with a pellet velocity of about 1 km/s. Further studies should include a correct model for transport of deuterium line radiation which will allow us to determine the density limits for runaway electron formation.

References

[1] ITER Interim Design Report, 1995.
[2] B.V. Kuteev, V.Yu. Sergeev and S. Sudo, Nucl. Fusion 35 (1995) 1167.
[3] F.L. Hinton and R.D. Hazeltine, Rev. Mod. Phys. 48 (1976) 239.
[4] R. Clark, J. Abdallah and D. Post, J. Nucl. Mater. 220 (1995) 1028.
[5] R.K. Janev, D. Post, W. Langer, K. Evans, D. Heitetz et al., J. Nucl. Mater. 121 (1984) 10.